

Adsorption of Cd(II) ions from aqueous solution by wasted low-grade phosphorus-containing oolitic hematite: equilibrium, kinetics, and thermodynamics

Xiaoli Yuan*, Dongshan Zhou*, Wentang Xia, Juan An, Xuejiao Zhou, Jianguo Yin

School of Metallurgy and Material Engineering, Chongqing University of Science and Technology, Chongqing 401331, China, Tel./Fax: +862365023436; email: yuanxiaoli1981@126.com (X. Yuan), 1179651333@qq.com (D. Zhou), wentangx@163.com (W. Xia), anjuan2692@126.com (J. An), zxxj040203017@126.com (X. Zhou), yjg06@163.com (J. Yin)

Received 30 August 2019; Accepted 22 February 2020

ABSTRACT

Low-grade phosphorus-containing oolitic hematite (LGPOH), an industrial solid waste generated in mining oolitic hematite with high phosphorus, was used as an adsorbent to remove Cd(II) ion from aqueous solution. Characteristics of LGPOH were comprehensively revealed by X-ray diffraction, scanning electron microscopy, and nitrogen adsorption Brunauer–Emmett–Teller method. Zeta potential and Fourier transform infrared spectrophotometer were used to elucidate the Cd(II) ion adsorption mechanism of LGPOH. The adsorption equilibrium, kinetics, and thermodynamics of Cd(II) ion onto LGPOH were studied. The results indicate that the optimum pH value for Cd(II) ion adsorption is 6.1, and the Cd(II) ion adsorption capacity reaches 9.56 mg/g at this pH value. At low pH (<6.1), the Cd(II) ion adsorption on LGPOH is mainly dominated by the complexation reaction process. When pH value is above 6.1, chemical precipitation plays a critical role in Cd(II) ion removal. The removal of Cd(II) ion by LGPOH is rapid, and the Cd(II) adsorption capacity exceeds 98% of the saturated adsorption capacity within 10 min. The adsorption kinetics of Cd(II) ion adsorption onto LGPOH follows the pseudo-second-order model. Moreover, the equilibrium adsorption data of Cd(II) ion adsorption onto LGPOH fits well with Langmuir isothermal model. The maximum adsorption capacity obtained from the Langmuir isotherm is 55.37 mg/g at 50°C. The calculated thermodynamic parameters reveal that the adsorption process of Cd(II) ion onto LGPOH is spontaneous and endothermic. Due to the cost-effective adsorption capability, LGPOH could be a promising adsorbent for Cd(II) ion removal from wastewater.

Keywords: Low-grade phosphorus-containing oolitic hematite (LGPOH); Cd(II) ion adsorption; Surface complexation; Endothermic; Kinetics; Thermodynamics

1. Introduction

During the past decades, more and more heavy metals (Cd, Pb, Cr, Hg, As, U, Th, etc.) were discharged into water bodies, which caused a serious environmental problem worldwide. Cd has been regarded as one of the most toxic heavy metals released into the environment, and it extensively exists in the effluents of pigment and battery production, metal and cement production, petrochemical

complexes industries [1–3]. The concentration of Cd(II) ion exceeding 0.003 mg/L in drinking water may cause human diseases like high blood pressure, kidney damage, diarrhea, cancer, etc. [4,5]. Nowadays, Cd(II) ion removal from wastewater has become an extremely urgent worldwide mission.

Various separation techniques including ion exchange, coagulation, ultrafiltration, chemical precipitation, reverse osmosis, flocculation, solvent extraction, and adsorption

* Corresponding authors.

have been developed for heavy metals ion removal [6–13]. Specially, the adsorption method is recognized as a highly promising technique for wastewater with low Cd(II) ion concentrations. As a conventional adsorbent for the pollutants removal from wastewater, commercial activated carbon is characterized by a good adsorption performance [14]. However, the high associated cost restricts the widespread use of this adsorbent. Therefore, many efforts have been paid to develop low-cost adsorbents in recent years, such as agricultural waste, grafted silica, petiolar felt-sheath of palm, olive stone waste, natural compost, peanut shell, natural kaolinite clay, kaolin, goethite, walnut shell, bone, waste Fe(III)/Cr(III) hydroxide, biomass, etc. [15–22]. The major advantages of using industrial by-products or natural materials for Cd(II) ion wastewater treatment are chemical stability (low solubility), low-cost, easy accessibility, and environmental friendliness.

Oolitic hematite with high phosphorus is an important type of iron ore resource. Mining this ore generates a phosphorus-containing industrial solid waste, low-grade phosphorus-containing oolitic hematite (LGPOH). LGPOH is becoming a serious environmental problem in the world due to the fact that it not only causes a landslide and dust pollution but also occupies the land resources. Hence, the treatment and recycling of LGPOH become an urgent mission. Our previous work indicates that LGPOH has a good Cd(II) ion adsorption performance [23]. However, the characteristics and mechanism of Cd(II) ion adsorption onto LGPOH, as well as the Cd(II) ion adsorption isotherm, kinetics, and thermodynamics are still unknown. In-depth understanding of these issues is very important for the economic and efficient utilization of LGPOH in the field of Cd(II) ion removal from wastewater.

In present work, several kinetic models (including the Elovich model, pseudo-first-order model, intra-particle diffusion model, and pseudo-second-order model) are used to describe the kinetic experimental data. The Langmuir and Freundlich isothermal models are applied to evaluate the adsorption equilibrium of Cd(II) ion onto LGPOH. Corresponding kinetic, isothermal, and thermodynamic parameters are then calculated. Furthermore, adsorption mechanisms of Cd(II) ions removal by LGPOH were also studied.

2. Materials and experimental procedure

LGPOH collected from the by-product in mining oolitic hematite with high phosphorus (Wushan, Chongqing, China) was used as an adsorbent in this research. The particle size of LGPOH adsorbent is less than 0.25 mm. The chemical composition analysis conducted by using X-ray fluorescence (XRF) (Model Lab Center XRF-1800, Shimadzu, Japan) indicates that LGPOH is mainly composed of Fe, SiO₂, CaO, MgO, Al₂O₃, P, etc., as listed in Table 1.

Adsorption experiments were executed according to the following procedures. First, a stock solution with Cd(II) ion concentration of 1,000 mg/L was prepared by dissolving a certain amount of chemically pure CdCl₂·2.5H₂O in deionized water. Then, aqueous solutions with designed Cd(II) ion concentrations of 30–70 mg/L were acquired by diluting defined volume of Cd(II) ion stock solution in 150 mL glass

Table 1
Chemical composition of LGPOH

Component	Content (wt.%)
TFe	31.29
SiO ₂	14.13
CaO	6.76
MgO	3.14
Al ₂ O ₃	3.55
P	1.26

round-bottom flasks immersed in a thermostatic shaker bath, adding the appropriate volume of 0.1 mol/L HCl or NaOH to adjust the pH value of the solution. Defined amounts of adsorbent were subsequently added to the flasks. The mixtures were stirred at 290 rounds per minute (rpm). Liquid samples collected at various time intervals were filtered, and the filtrate was collected for subsequent Cd(II) ion analysis [24].

Adsorption experiments to explore the effect of initial pH value on Cd(II) ion adsorption was examined at 20°C, fixing LGPOH dosage, initial Cd(II) ion concentration and adsorption time to 10 g/L, 30 mg/L, and 5 min, respectively. Cd(II) ion adsorption isotherms were investigated at four different temperatures (20°C, 30°C, 40°C, and 50°C) for 10 min with the initial Cd(II) ion concentration varying from 30 to 70 mg/L, and LGPOH dosage and pH value were fixed to 20 g/L and 6.1, respectively. To evaluate the Cd(II) ion adsorption kinetics, adsorption experiments were executed for 5–40 min at 30°C, with different initial Cd(II) ion concentrations (30, 40, 50, 60, and 70 mg/L) as well as fixed LGPOH dosage of 20 g/L and initial pH value of 6.1.

The Cd(II) ion concentration of samples was analyzed by flame atomic absorption spectrophotometry method (Model TAS-986, Puxi, China) to follow the Cd(II) ion adsorption onto LGPOH. A pH meter (Model FE28-Standard, Mettler-Toledo, Switzerland) was used to measure the pH value of the aqueous solution. The phase composition of LGPOH was conducted by X-ray diffraction (XRD) (Model D/max 2500 PC, Rigaku, Japan) with Cu Ka radiation. The thermal stability of LGPOH was evaluated by thermogravimetry (TG) analysis (Model STA 449C, Netzsch Co. Ltd., Germany) in the air at a heating rate of 5°C/min until 1,200°C. The microstructure of LGPOH was observed by scanning electron microscopy (SEM) (Model JSM-7800F, JEOL, Japan). The zeta potentials of LGPOH samples before and after adsorption were measured using a zeta potential analyzer (Model CoulterDelsa440sx, Beckman Coulter, USA) in the pH range 1.5–12.0 by the similar method reported in our previous work [25]. The element composition of the surface of LGPOH after adsorption was characterized by energy-dispersive X-ray (EDX) spectroscopy (Model X-Max, Oxford Instruments, UK) attached to SEM. The particle size distribution and specific surface area of LGPOH were measured using the nitrogen adsorption Brunauer–Emmett–Teller (BET) method by laser diffraction particle size analyzer (LDPSA) (Model MS 2000, Malvern, USA). Infrared (IR) spectroscopy measurements of LGPOH before and after adsorption were implemented on a Fourier

transform infrared (FTIR) spectrophotometer (Model 5DXC, Nicolet Co., USA) at room temperature.

3. Results and discussion

3.1. Characteristics of LGPOH

The XRD pattern of LGPOH (Fig. 1) indicates that the main crystalline phases in LGPOH are hematite, dolomite, and quartz. In addition, a minor amount of fluorapatite, rodolicoite, and calcium phosphate have existed in LGPOH. Fig. 2 shows the TG curve of LGPOH, the obvious weight loss from $\sim 500^{\circ}\text{C}$ to $\sim 750^{\circ}\text{C}$ is caused by the decomposition of dolomite. Fig. 3 presents the typical SEM images of LGPOH powders. It can be seen from Fig. 3a (image with low magnification) that the particle size of LGPOH is very heterogeneous. Besides, microstructure observation with high magnification indicates LGPOH is characterized by a porous structure and rough surface, and numerous fine LGPOH particles are aggregated on the surface of the coarse LGPOH particle, as shown in Fig. 3b. Based on the result of LDPSA, the average particle size and specific surface area of

LGPOH adsorbent are $40.9\ \mu\text{m}$ and $0.916\ \text{m}^2/\text{g}$, respectively. In addition, it can be seen from Fig. 4 that the particle size distribution of LGPOH powder is broad, and the volume fractions of LGPOH particles with a size less than $1\ \mu\text{m}$, between 1 and $100\ \mu\text{m}$ and more than $100\ \mu\text{m}$ are about 4.0%, 89.5%, and 6.5%, respectively.

3.2. Effect of initial pH value on Cd(II) ion adsorption

It is well known the adsorption characteristic and capacity of Cd(II) ion onto the adsorbents is highly dependent on the solution pH. Fig. 5 shows the plot of Cd(II) ion removal capacity vs. initial pH value. The Cd(II) ion adsorption capacity increased rapidly from 7.70 to 9.56 mg/g when the pH value increased from 1.5 to 6.1. Further increasing pH introduces a continuous decrease of Cd(II) ion adsorption capacity.

At low pH (<6.1), the main form of Cd(II) is Cd^{2+} . Meanwhile, the protonation of adsorbent is given rise by the high concentration of H^+ , which causes the rejection of Cd^{2+} , thereby, leads to competition and repulsion between H^+ and Cd(II) ions for active sites on the surface of adsorbent [26]. In present work, when the pH varies from 1.5 to 6.1,

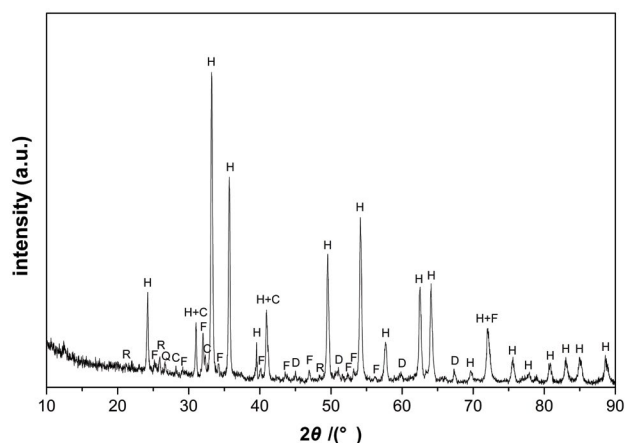


Fig. 1. XRD pattern of LGPOH (H is hematite, D is dolomite, F is fluorapatite, C is calcium phosphate, R is rodolicoite, Q is quartz).

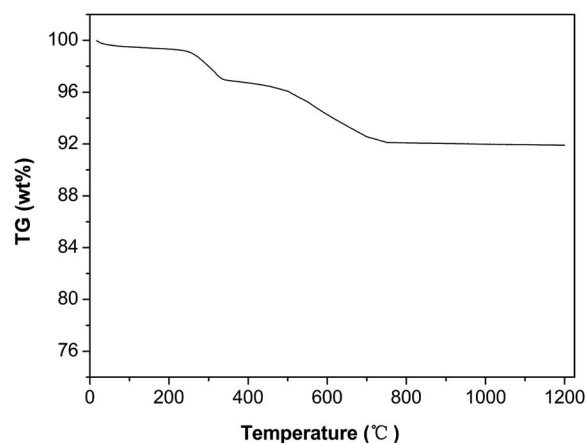


Fig. 2. TG curve of LGPOH.

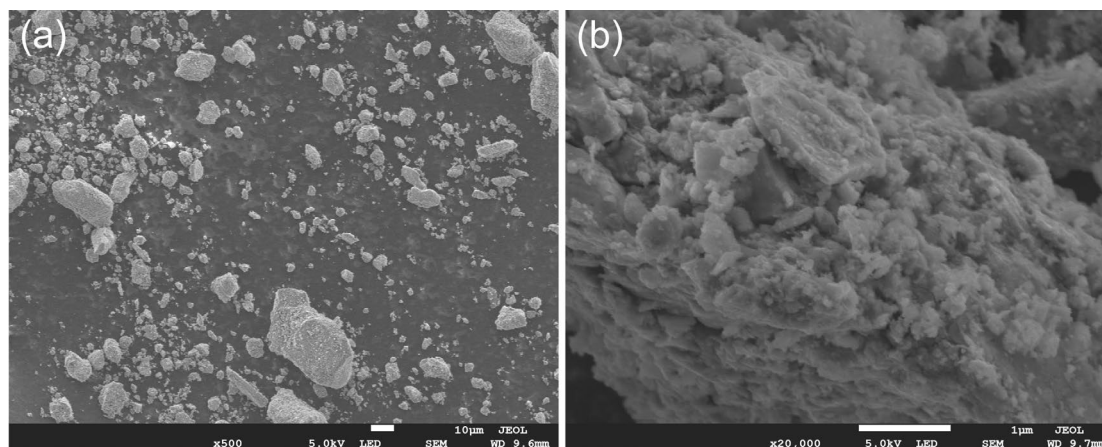


Fig. 3. SEM micrographs of LGPOH at different magnifications (a) $500\times$ and (b) $20,000\times$.

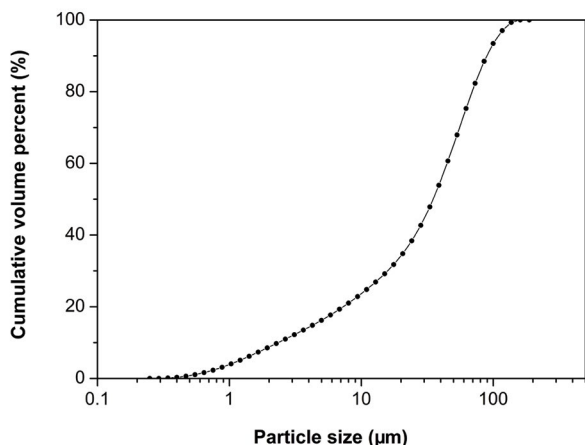


Fig. 4. Particle size distribution of LGPOH.

the protonation of LGPOH is weakened. Therefore, more Cd(II) ions can get access to adsorption sites, which favors the hydroxy complexes absorption, and so raises Cd(II) ions adsorption capability of LGPOH. However, as the pH ranges at 6.1–12.0, hydroxide compound ($\text{Cd}(\text{OH})_2$) precipitate becomes the dominating species of Cd(II) [27–30], therefore, pH value increases introduces the decrease of Cd(II) ion removal capacity.

3.3. Adsorption mechanism analysis

Fig. 6 shows the relationships between zeta potential and initial pH for the LGPOH samples before and after adsorption (adsorption experiment was conducted at 20°C for 72 h to ensure the achievement of adsorption equilibrium, fixing LGPOH dosage and initial Cd(II) ion concentration to 10 g/L and 30 mg/L, respectively). For the sample before adsorption, the isoelectric point (IEP_{pH}) value is 2.4. After the adsorption process, the IEP_{pH} value increases to 3.4. In addition, it is clear that the LGPOH becomes more positively charged after Cd^{2+} adsorption in the examined pH range. The above results imply the adsorption process is chemical adsorption, and the electrostatic repulsion action might prejudice the adsorption. Moreover, it can be seen from Fig. 6 that the zeta potential of the LGPOH sample before adsorption decreases sharply (from 7.37 to -17.07 mV) with the initial pH increasing from 1.5 to 6.0. However, as the initial pH further increases, the zeta potential decreases slowly. The rapid decrease of zeta potential induced by pH increasing at pH 1.5–6.0 may be attributed to the fact that higher pH value promotes the formation of negatively charged hydroxyl groups on the surface of LGPOH. These hydroxyl groups are active sites for Cd^{2+} adsorption. Hence, it could be concluded that the enhancement of the negatively charged hydroxyl group formation is also the main factor contributed to the rapid increase of Cd(II) ion removal capacity with pH value increasing at pH 1.5–6.1 as presented in Fig. 5.

Metal sorption is closely related to the specific surface of the adsorbent [31]. Previous works suggested that surfaces of oxide usually coordinate water molecules in aqueous suspension [25,32]. As mentioned above, LGPOH has

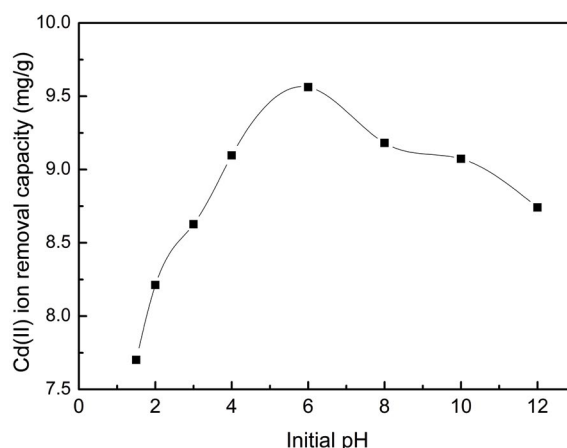


Fig. 5. Effect of pH on Cd(II) ion adsorption on LGPOH, where the initial LGPOH dosage, Cd(II) ion concentration, adsorption time, and adsorption temperature were fixed to 10 g/L, 30 mg/L, 5 min, and 20°C, respectively.

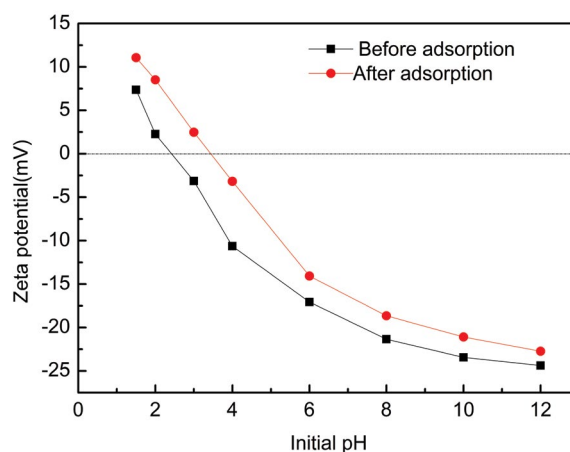


Fig. 6. Relationship between Zeta potential of LGPOH and initial pH, where the initial LGPOH dosage, Cd(II) ion concentration, adsorption time, and adsorption temperature were fixed to 10 g/L, 30 mg/L, 72 h, and 20°C, respectively.

a high amount of oxides including hematite, dolomite, and quartz. Hence, surface hydroxyl groups will form on the LGPOH surfaces. Then, the characteristics of these functional groups will strongly influence the adsorption of Cd(II) ion onto the LGPOH. Therefore, hydroxyl groups on the surfaces of LGPOH samples before and after adsorption were revealed by FTIR spectra (Fig. 7). The adsorption experiment was carried out at 20°C for 5 min, fixing the initial Cd(II) ion concentration, LGPOH dosage, and initial pH value to 30 mg/L, 10 g/L, and 6.1, respectively. The valleys at 3,289 and 3,086 cm^{-1} in Fig. 7 are corresponding to the bending and stretching vibrations of H–O–H (physisorbed water molecule) [25,31]. In addition, three bands at 1,020, 744, and 535 cm^{-1} are observed in Fig. 7, which could be attributed to the formation of multicentered hydroxyl group S–OH (where S represents a central ion of the mineral surface) [31]. For the sample after adsorption, two new bands (at 918

and 694 cm^{-1}) appear. The new bands may arise from the formation of the inner-sphere surface complex (S-O-Cd) due to the reaction of Cd(II) ion and adsorbent. Based on the above results, the adsorption mechanism of Cd(II) ion onto LGPOH at low pH can be described as Eqs. (1)–(3).

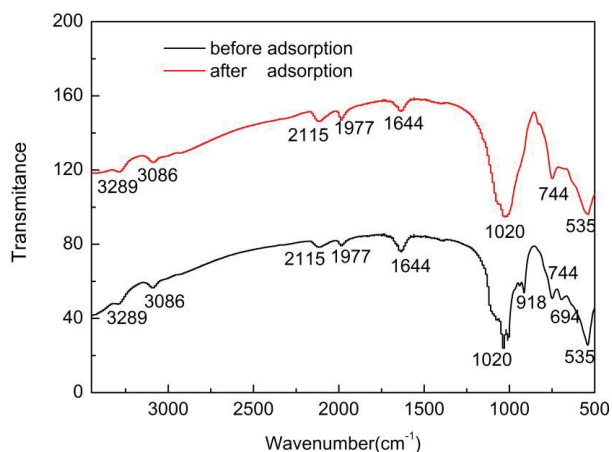


Fig. 7. FTIR spectra of LGPOH samples before and after Cd(II) ion adsorption, where the Cd(II) ion adsorption initial pH, the temperature, LGPOH dosage, the initial Cd(II) ion concentration, and adsorption time were fixed to 6.1, 20°C , 10 g/L, 30 mg/L, and 5 min, respectively.



Fig. 8 illustrates the above-proposed mechanism for Cd(II) ion adsorption process. Obviously, Cd(II) ion adsorption at low pH (<6.1) would occur at the aqueous Cd(II) ion/LGPOH interface, which implies that the replacement of surface hydroxyl groups by the Cd(II) ions (complexation) is the predominant adsorption mechanism.

3.4. Characterization of a product after adsorption

Figs. 9a and b show the SEM micrographs of the LGPOH sample after adsorption (the sample is the same with that of the FTIR test). Compared with the sample before adsorption, no significant variation in the morphology can be observed. However, the sample after Cd(II) adsorption is slightly more aggregated. BET result indicates the specific surface area increases slightly to $0.982\text{ m}^2/\text{g}$ after Cd(II) adsorption, which can be attributed to the fact that aggregates with the more porous structure are formed after Cd(II) adsorption. To further confirm the Cd(II) adsorption onto LGPOH, EDX analysis of LGPOH after adsorption was performed. As shown in Fig. 9c, a certain amount of cadmium is evidenced, which confirms the successful adsorption of Cd(II) by LGPOH.

3.5. Cd(II) ion adsorption kinetics

Fig. 10 shows the plots of the Cd(II) adsorption capacity of LGPOH vs. adsorption time at various initial Cd(II) ion concentrations. It can be seen that the Cd(II) adsorption is very fast initially. As shown in Fig. 10, the Cd(II) adsorption

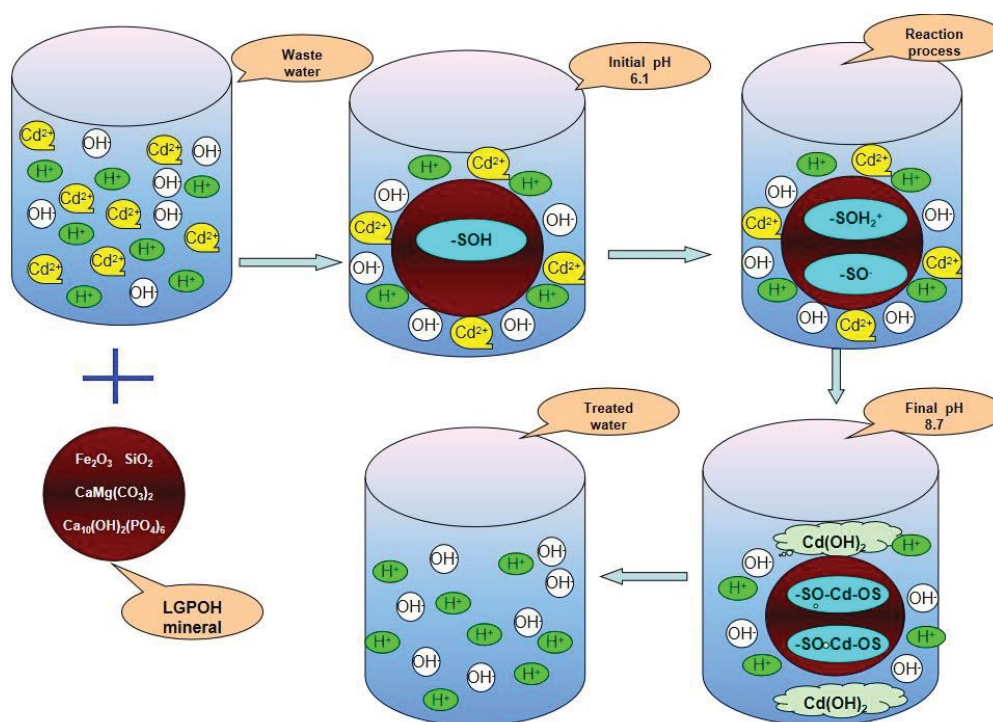


Fig. 8. Schematic diagram of the major mechanism of adsorption Cd(II) ion onto the surface of LGPOH.

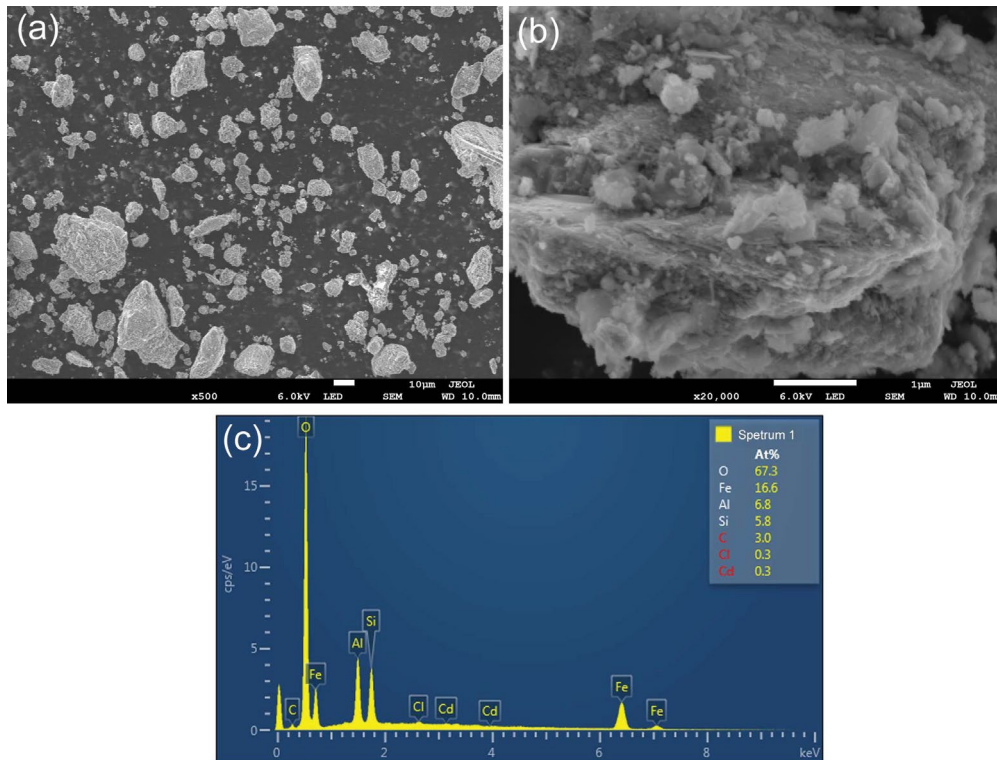


Fig. 9. SEM micrographs (a) 500 \times , (b) 20,000 \times , and (c) EDX spectrum of LGPOH sample after adsorption.

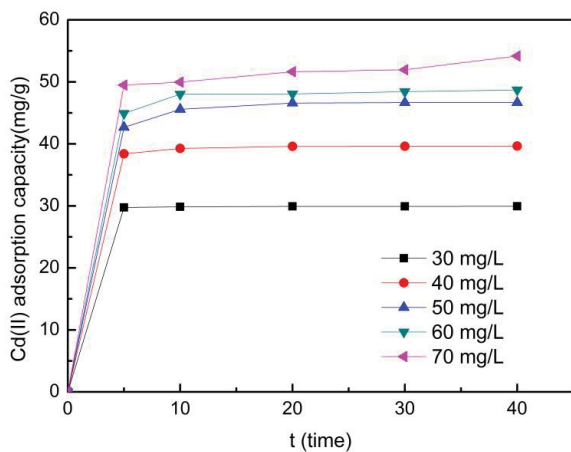


Fig. 10. Variation of adsorption capacity of LGPOH with adsorption time at different initial Cd(II) ion concentrations, where the adsorption temperature, LGPOH dosage, and initial pH were fixed to 30°C, 20 g/L, and 6.1, respectively.

capacity exceeds 98% of the saturated adsorption capacity within 10 min. The rapid adsorption during the incipient stage may be attributed to a large number of adsorption sites and a high solute concentration gradient. With the reaction further progressing, Cd(II) ion concentration and availability of adsorption sites are reduced, thus decreasing Cd(II) ion uptake rate.

To clarify the rate-controlling step of the Cd(II) ion adsorption process, four kinetics models, including the Elovich

model, pseudo-first-order model, intra-particle diffusion model, and pseudo-second-order model, were employed to investigate Cd(II) ion adsorption kinetics performance. The above kinetics models are described by the following Eqs. (4)–(7), respectively [33–36]:

Elovich model:

$$Q_t = \frac{1}{\beta} \ln(\alpha\beta) + \frac{1}{\beta} \ln t \quad (4)$$

Pseudo-first-order model:

$$\frac{1}{Q_i} = \frac{k_1}{Q_f t} + \frac{1}{Q_f} \quad (5)$$

Intra-particle diffusion model:

$$Q_t = c + k_m t^{1/2} \quad (6)$$

Pseudo-second-order model:

$$\frac{t}{Q_i} = \frac{1}{k_2 Q_f^2} + \frac{t}{Q_f} \quad (7)$$

where Q_f (mg/g) and Q_t (mg/g) are the adsorption capacities at equilibrium and a certain adsorption time t (min), respectively; α (mg/(g min)) is the initial adsorption rate constant and β (g/mg) is a parameter related to the extent of surface coverage and activation energy for chemisorption; k_1 (min⁻¹), k_2 (g/(mg min)) and k_m (mg/(g min^{0.5})) are the rate

constants of the pseudo-first-order model, pseudo-second-order model, and intra-particle diffusion model, respectively; c is a parameter obtained from the intercept when fitting the adsorption data by an intra-particle diffusion model.

Fig. 11 shows the plots obtained by fitting experimental results using the above four kinetics models. In addition, the corresponding rate constants, and the correlation coefficient (R^2) are summed up in Table 2. It can be seen that the R^2 value of fitted plots corresponding to the pseudo-second-order model is very high (>0.998), which is higher than those corresponding to the other three models. Therefore, it can be concluded that the adsorption kinetics satisfied the pseudo-second-order kinetic model, which implies that the chemical sorption reaction is the rate-limiting step [37]. Hence, the amount of active sites on the LGPOH surface determines the Cd(II) adsorption capacity of LGPOH [38]. This phenomena have also been observed in the adsorption of Cd(II) ion on bentonite $\text{Fe}_3\text{O}_4\text{-MnO}_2$ composite [39], raw attapulgite clay, and waste-struvite/attapulgite [40], modified steel-making slag [41] and nickel aluminum layered double hydroxide [42].

3.6. Cd(II) ion adsorption isotherm

Fig. 12 shows the adsorption isotherm results at different temperatures. Obviously, the adsorption capacity of Cd(II) ion increases with the temperature rising from 20°C to 50°C. The result indicates that the Cd(II) ion adsorption onto LGPOH is characterized by an endothermic reaction. Thus the higher temperature favors Cd(II) ion removal by LGPOH.

As well known, the Cd(II) ion adsorption ability and performance of the adsorbent can be revealed by adsorption isotherm models [43,44]. In present work, the Langmuir and Freundlich models were used in the isotherm study. Eqs. (8) and (9) are the linear expressions of Langmuir and Freundlich models, respectively [45,46]:

$$\frac{C_f}{Q_f} = \frac{1}{bQ_{\max}} + \frac{C_f}{Q_{\max}} \quad (8)$$

$$\log Q_f = \log k + \frac{\log C_f}{n} \quad (9)$$

where Q_f (mg/g) is the Cd(II) ion concentration in the solid adsorbent, C_f (mg/L) is the equilibrium Cd(II) ion concentration in the solution, k ($\text{mg}^{1-1/n}\text{L}^{1/n}/\text{g}$) and n are constants related to the adsorption capacity and the energy of adsorption, respectively; Q_{\max} (mg/g) is the maximum adsorption capacity, β (L/mg) is a constant related to the energy of adsorption.

The adsorption isotherm data of Fig. 12 were fitted to the Langmuir and Freundlich models. The results are illustrated in Figs. 13a and b, respectively. Table 3 lists the isotherm constants and correlation coefficient (R^2). High R^2 values of the Langmuir model indicate that the isothermal of Cd(II) ion adsorption on the LGPOH follows the Langmuir equation. In addition, Q_{\max} obtained by Langmuir model in Table 3 suggests that LGPOH possess

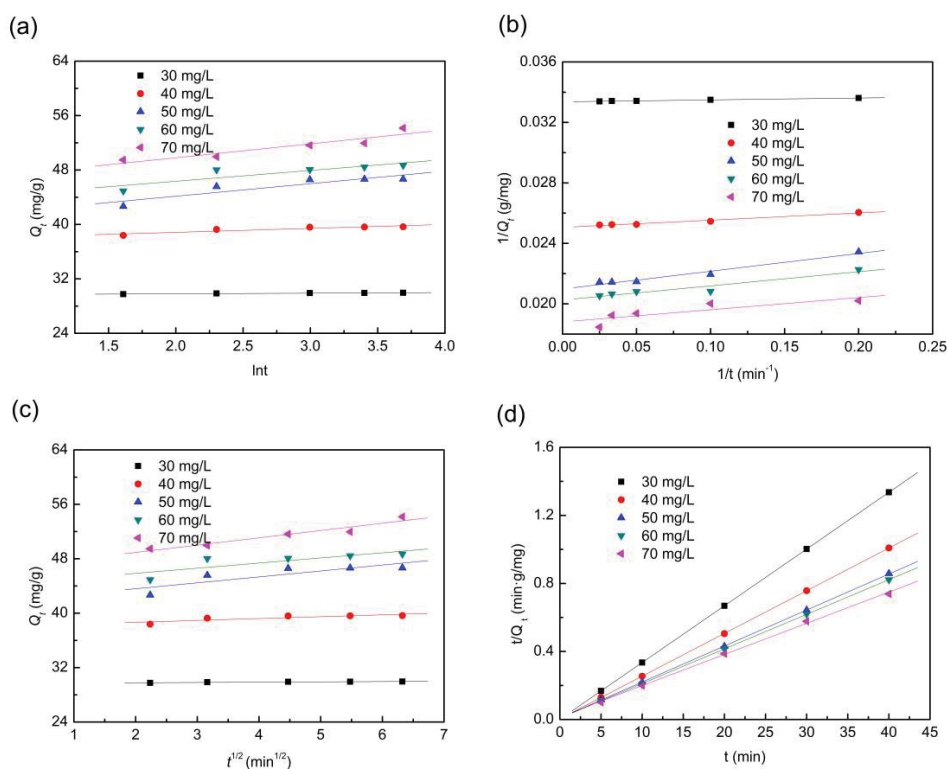


Fig. 11. Linearized form plots of different kinetic models for Cd(II) ion adsorption on LGPOH. (a) Elovich model, (b) pseudo-first-order model, (c) intra-particle diffusion model, and (d) pseudo-second-order model; the adsorption experiments were carried out with fixing the initial pH, adsorption temperature and LGPOH dosage to 6.1, 30°C, and 20 g/L, respectively.

Table 2
Estimated kinetic model parameters for Cd(II) ion adsorption on LGPOH

Elovich model: $Q_t = \frac{1}{\beta} \ln(\alpha\beta) + \frac{1}{\beta} \ln t$				
Initial Cd(II) ion concentration (mg/L)	α (mg/(g min))	β (g/mg)	R^2	SD
30	0.093	10.820	0.9331	0.0241
40	0.587	1.729	0.8442	0.2423
50	1.933	0.542	0.8259	0.8270
60	1.655	0.627	0.7640	0.8644
70	2.138	0.489	0.8663	0.7835
Pseudo-first-order model: $\frac{1}{Q_t} = \frac{k_1}{Q_f t} + \frac{1}{Q_f}$				
Initial Cd(II) ion concentration (mg/L)	k_1 (min ⁻¹)	Q_e (mg/g)	R^2	SD
30	0.038	29.967	0.9960	0.0001
40	0.191	39.904	0.9784	0.0001
50	0.560	47.664	0.9681	0.0002
60	0.463	49.383	0.9150	0.0002
70	0.429	53.192	0.7067	0.0004
Intra-particle diffusion model: $Q_t = c + k_m t^{1/2}$				
Initial Cd(II) ion concentration (mg/L)	c	k_m (mg/(g min ^{0.5}))	R^2	SD
30	29.684	0.045	0.8515	0.0360
40	38.116	0.274	0.7343	0.3165
50	41.852	0.871	0.7116	1.0645
60	44.354	0.754	0.6612	1.0358
70	46.781	1.074	0.9269	0.5794
Pseudo-second-order model: $\frac{t}{Q_t} = \frac{1}{k_2 Q_f^2} + \frac{t}{Q_f}$				
Initial Cd(II) ion concentration (mg/L)	k_2 (g/(mg min))	Q_e (mg/g)	R^2	SD
30	0.863	29.976	1.0000	0.0002
40	0.165	39.809	1.0000	0.0008
50	0.051	47.237	0.9999	0.0025
60	0.053	49.116	0.9999	0.0023
70	0.021	54.585	0.9988	0.0103

a high monolayer adsorption capacity, which supports the possibility of the adsorption mechanism mentioned above.

In order to assess the Cd(II) ion adsorption capacity of LGPOH, the maximum Cd(II) ion adsorption capacities of different adsorbents are compared as listed in Table 4. The maximum adsorption capacity (Q_{max}) of LGPOH is 55.37 mg/g at 50°C, and it is about 42.59 times of the adsorption capacity of calcitic limestone [47], 3.08, 12.64, and 1.80 times of the adsorption capacities of red mud [48], kaolin [49] and manganoxide mineral [50], respectively. Though the adsorption capacity of graphene oxides for Cd(II) ion was reported as 111.11 mg/g which is much over 55.37 mg/g determined in this study, the application of graphene oxides is limited by the high associated cost adsorbent. Thus, comprehensively considering the cost and adsorption capacity,

LGPOH is a promising adsorbent for the removal of Cd(II) ion.

3.7. Thermodynamic parameters of adsorption

Adsorption isotherm results indicate Cd(II) ion adsorption on the LGPOH is an endothermic reaction. To further ascertain the effect of temperature on the Cd(II) ion adsorption, thermodynamic parameters including standard free energy change (ΔG), standard enthalpy change (ΔH), and standard entropy change (ΔS) were determined.

The calculation Eq. (10) of ΔG is as follows:

$$\Delta G = -RT \ln K \quad (10)$$

where R is the gas constant, T (K) is the temperature, and K is the equilibrium constant which is numerically approximated the Langmuir constant b [54]. Thermodynamic parameters of ΔH and ΔS are evaluated by the following equation from the intercept and slope of ΔG against T (Fig. 14) [55]:

$$\Delta G = \Delta H - T\Delta S \tag{11}$$

Table 5 lists the values of ΔG , ΔH , and ΔS for the adsorption of Cd(II) ion onto LGPOH. It can be seen the values of ΔG are all negative at the three different temperatures (30°C,

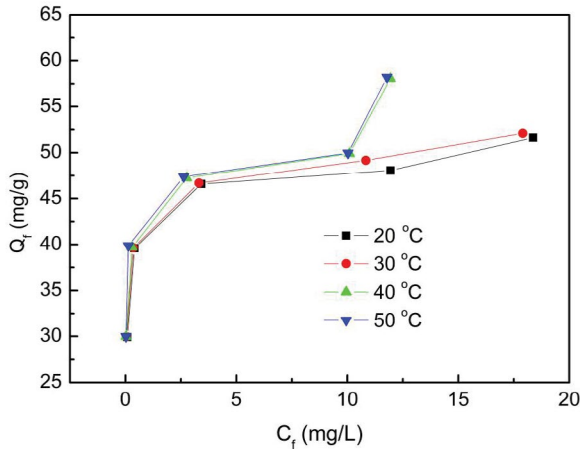


Fig. 12. Adsorption isotherm of Cd(II) ion by LGPOH at different temperatures, where the initial pH, adsorption time and LGPOH dosage were fixed to 6.1, 10 min, and 20 g/L, respectively, and the initial Cd(II) ion concentration varies from 30 to 70 mg/L.

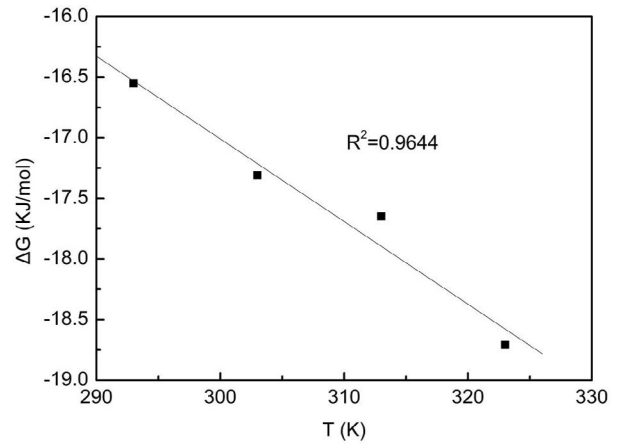


Fig. 14. Plot of ΔG vs. T for Cd(II) ion adsorption by LGPOH, where the initial pH, adsorption time and LGPOH dosage were fixed to 6.1, 10 min, and 20 g/L, respectively, and the initial Cd(II) ion concentration varied from 30 to 70 mg/L.

Table 3
Estimated isotherm parameters for Cd(II) ion adsorption on LGPOH

Temperature (°C)	Langmuir isotherm: $\frac{C_f}{Q_f} = \frac{1}{bQ_{max}} + \frac{C_f}{Q_{max}}$				Freundlich isotherm: $\log Q_f = \log k + \frac{\log C_f}{n}$			
	b (L/mg)	Q_{max} (mg/g)	R^2	SD	k ($\text{mg}^{-1/n}\text{L}^{1/n}/\text{g}$)	$1/n$	R^2	SD
20	4.270	51.230	0.9980	0.0080	39.973	0.091	0.9341	0.0280
30	4.319	51.948	0.9987	0.0061	41.061	0.087	0.9686	0.0198
40	4.661	55.279	0.9883	0.0128	42.924	0.098	0.9562	0.0265
50	5.125	55.371	0.9883	0.0136	44.004	0.089	0.9238	0.0351

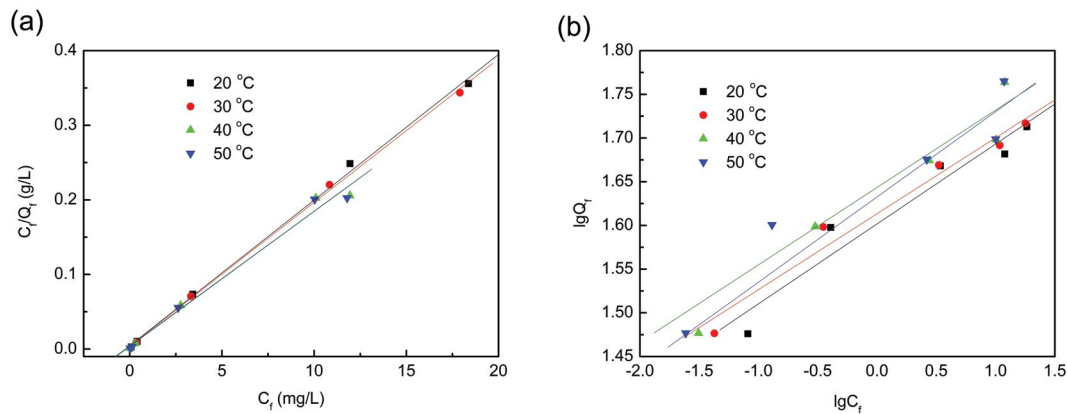


Fig. 13. Linearized form plots of isotherm for Cd(II) ion adsorption on LGPOH: (a) Langmuir isotherm and (b) Freundlich isotherm, where the initial pH, adsorption time and LGPOH dosage were fixed to 6.1, 10 min, and 20 g/L, respectively, and the initial Cd(II) ion concentration varied from 30 to 70 mg/L.

Table 4

Comparison of the maximum Cd(II) ion capacities of different adsorbents and the corresponding adsorption conditions

No..	Material	pH	Temperature (°C)	Adsorption capacity (mg/g)	References
1	Red mud	6.5	25	17.98	[51]
2	Na-bentonite	4.0	20	26.20	[47]
3	Kaolin	7.3	20	3.00	[49]
4	Kaolinite	5.5	50	4.38	[52]
5	Montmorillonite	5.5	30	30.70	[53]
6	Calcitic limestone	5.0	20	1.30	[47]
7	Turkish illitic clay	4.0	40	13.09	[9]
8	Manganoxide mineral	6.0	45	6.80	[50]
9	Clarified sludge	5.0	30	36.23	[26]
11	Graphene oxides	3.5	20	111.11	[31]
10	LGPOH	6.1	50	55.37	This study

Table 5

Thermodynamic parameters for the adsorption of Cd(II) ion on LGPOH

Temperature (K)	ΔG (KJ/mol)	ΔH (KJ/mol)	ΔS (J/mol K)
303	-16.55		
313	-17.31		
323	-17.65	0.0034	0.0681
333	-18.71		

40°C, and 50°C), which suggests the spontaneous nature of adsorption and the feasibility of the present adsorption process. In addition, the decrease in ΔG values with temperature increasing indicates that higher temperatures favor the adsorption of Cd(II) ion onto LGPOH. During the adsorption process, the water molecules are released from the hydrated ions and present on the surface of LGPOH [56], which increases the randomness at the solid-solution interface. So, the adsorption reaction shows a positive value of ΔS . Moreover, due to the endothermic nature of Cd(II) ion adsorption, the value of ΔH is positive.

4. Conclusions

A low-cost industrial waste, LGPOH was used as an adsorbent to remove Cd(II) ion from aqueous solution. The effect of pH value on Cd(II) ion adsorption capacity was investigated, and the adsorption mechanisms were discussed. Moreover, the Cd(II) ion adsorption kinetics, isotherm, and thermodynamics were evaluated. The following conclusions were drawn:

- The adsorption efficiencies of Cd(II) ion onto LGPOH are strongly dependent on the pH value of the solution. A relatively high Cd(II) ion adsorption efficiency was obtained at a pH of 6.1. When pH value is in the range of 1.5–6.1, Cd(II) ion adsorption onto LGPOH follows a complexation mechanism, while the chemical precipitation played an important role in Cd(II) ion removal as pH is above 6.1.

- The Cd(II) ion adsorption onto LGPOH in aqueous solution is rapid and the adsorption kinetics can be well described by the pseudo-second-order kinetic model. The Cd(II) ion adsorption onto LGPOH is mainly controlled by chemisorption, which is the rate-determining step.
- Higher temperature favors the adsorption of Cd(II) ion onto LGPOH. The equilibrium adsorption data for Cd(II) ion is well fitted by the Langmuir adsorption isotherm model. The maximum adsorption capacity of LGPOH for the Cd(II) ion is 55.37 mg/g at 50°C. Further thermodynamic studies proved that the Cd(II) ion adsorption on LGPOH is spontaneous and endothermic.
- LGPOH is a cost-effective adsorbent for the removal of Cd(II) ion from aqueous solution, due to its low-cost and high adsorption capability.

Acknowledgments

This research was funded by Project Supported by the Scientific and Technological Research Program of Chongqing Municipal Education Commission (Grant No.KJQN201801507) and the Chongqing Science and Technology Commission in China (Grant No.cstc2019jcyj-msxmX0132). This work was also financially supported by the National Natural Science Foundation of China (Grant No.51504051, 51174246, 51674057, 51904052 and 51574053).

References

- [1] H. Sharififard, Z.H. Shahraki, E. Rezvanpanah, S.H. Rad, A novel natural chitosan/activated carbon/iron bio-nanocomposite: sonochemical synthesis, characterization, and application for cadmium removal in batch and continuous adsorption process, *Bioresour. Technol.*, 270 (2018) 562–569.
- [2] D. Rahangdale, A. Kumar, Acrylamide grafted chitosan-based ion-imprinted polymer for the recovery of cadmium from nickel-cadmium battery waste, *J. Environ. Chem. Eng.*, 6 (2018) 1828–1839.
- [3] C. Jeon, The adsorption behavior of cadmium ions from aqueous solution using pen shells, *J. Ind. Eng. Chem.*, 58 (2018) 57–63.
- [4] M. Basu, A.K. Guha, L. Ray, Adsorption behavior of cadmium on husk of lentil, *Process Saf. Environ. Prot.*, 106 (2017) 11–22.

- [5] S.S. Pillai, B. Deepa, E. Abraham, N. Girija, P. Geetha, L. Jacob, M. Koshy, Biosorption of Cd(II) from aqueous solution using xanthated nano banana cellulose: equilibrium and kinetic studies, *Ecotoxicol. Environ. Saf.*, 98 (2013) 352–360.
- [6] M. Naushad, A. Mittal, M. Rathore, V. Gupta, Ion-exchange kinetic studies for Cd(II), Co(II), Cu(II), and Pb(II) metal ions over a composite cation exchanger, *Desal. Water Treat.*, 54 (2015) 2883–2890.
- [7] M. Naushad, Z.A. Allothman, M.R. Awual, M.M. Alam, G.E. Eldesoky, Adsorption kinetics, isotherms, and thermodynamic studies for the adsorption of Pb²⁺ and Hg²⁺ metal ions from aqueous medium using Ti(IV) iodovanadate cation exchanger, *Ionics*, 21 (2015) 2237–2245.
- [8] M. Naushad, Z.A. Allothman, Separation of toxic Pb²⁺ metal from aqueous solution using strongly acidic cation-exchange resin: analytical applications for the removal of metal ions from pharmaceutical formulation, *Desal. Water Treat.*, 53 (2015) 2158–2166.
- [9] D. Ozdes, C. Duran, H.B. Senturk, Adsorptive removal of Cd(II) and Pb(II) ions from aqueous solutions by using Turkish illitic clay, *J. Environ. Manage.*, 92 (2011) 3082–3090.
- [10] M. Eloussaief, M. Benzina, Efficiency of natural and acid-activated clays in the removal of Pb(II) from aqueous solutions, *J. Hazard. Mater.*, 178 (2010) 753–757.
- [11] A.A. Alqadami, M. Naushad, Z.A. Allothman, A.A. Ghfar, Novel metal-organic framework (MOF) based composite material for the sequestration of U(VI) and Th(IV) metal ions from aqueous environment, *ACS Appl. Mater. Interfaces*, 9 (2017) 36026–36037.
- [12] I. Mironyuk, T. Tatarchuk, M. Naushad, H. Vasylyeva, I. Myktyyn, Highly efficient adsorption of strontium ions by carbonated mesoporous TiO₂, *J. Mol. Liq.*, 285 (2019) 742–753.
- [13] A. Mittal, M. Naushad, G. Sharma, Z.A. Allothman, S.M. Wabaidur, M. Alam, Fabrication of MWCNTs/ThO₂ nanocomposite and its adsorption behavior for the removal of Pb(II) metal from aqueous medium, *Desal. Water Treat.*, 57 (2016) 21863–21869.
- [14] E. Asuquo, A. Martin, P. Nzerem, F. Siperstein, X.L. Fan, Adsorption of Cd(II) and Pb(II) ions from aqueous solutions using mesoporous activated carbon adsorbent: equilibrium, kinetics and characterization studies, *J. Environ. Chem. Eng.*, 5 (2017) 679–698.
- [15] M. Ghasemi, M. Naushad, N. Ghasemi, Y. Khosravi-Fard, Adsorption of Pb(II) from aqueous solution using new adsorbents prepared from agricultural waste: adsorption isotherm and kinetic studies, *J. Ind. Eng. Chem.*, 20 (2014) 2193–2199.
- [16] M.Q. Jiang, X.Y. Jin, X.Q. Lu, Z.L. Chen, Adsorption of Pb(II), Cd(II), Ni(II), and Cu(II) onto natural kaolinite clay, *Desalination*, 252 (2010) 33–39.
- [17] C. Namasivayam, K. Ranganathan, Removal of Cd(II) from wastewater by adsorption on “waste” Fe(III)/Cr(III) hydroxide, *Water Res.*, 29 (1995) 1737–1744.
- [18] K. Kadirvelu, C. Namasivayam, Activated carbon from coconut coir pith as metal adsorbent: adsorption of Cd(II) from aqueous solution, *Adv. Environ. Res.*, 7 (2003) 471–478.
- [19] I. Kula, M. Ugurlu, M.H. Karaoglu, A. Celik, Adsorption of Cd(II) ions from aqueous solutions using activated carbon prepared from olive stone by ZnCl₂ activation, *Bioresour. Technol.*, 99 (2008) 492–501.
- [20] H.B. Michael, B. Bart, Modeling the sorption of Mn(II), Co(II), Ni(II), Zn(II), Cd(II), Eu(III), Am(III), Sn(IV), Th(IV), Np(V), and U(VI) on montmorillonite: linear free energy relationships and estimates of surface binding constants for some selected heavy metals and actinides, *Geochim. Cosmochim. Acta*, 69 (2005) 875–892.
- [21] C. Nathalie, G. Richard, D. Eric, Adsorption of Cu(II) and Pb(II) onto a grafted silica: isotherms and kinetic models, *Water Res.*, 37 (2003) 3079–3086.
- [22] G. Blazquez, F. Hernainz, M. Calero, L.F. Ruiz-Nunez, Removal of cadmium ions with olive stones: the effect of some parameters, *Process Biochem.*, 40 (2005) 2649–2654.
- [23] X.L. Yuan, W.T. Xia, J. An, X.Y. Xiang, X.J. Zhou, J.G. Yin, W.Q. Yang, Removal of Cd(II) Ion from Aqueous Solution by Adsorption on Wasted Low-Grade Phosphorus-Containing Iron Ore, 8th International Symposium on High-Temperature Metallurgical Processing, The Minerals, Metals & Materials Series, Springer, Cham, 2017, pp. 779–787.
- [24] X.L. Yuan, W.T. Xia, J. An, X.J. Zhou, X.Y. Xiang, J.G. Yin, W.Q. Yang, Adsorption characteristics of Pb(II) ions onto wasted iron ore tailing with phosphorus used as natural adsorbent from aqueous solution, *Desal. Water Treat.*, 98 (2017) 222–232.
- [25] X.L. Yuan, C.G. Bai, W.T. Xia, J. An, Acid-base properties and surface complexation modeling of phosphate anion adsorption by wasted low-grade iron ore with high phosphorus, *J. Colloid Interface Sci.*, 428 (2014) 208–213.
- [26] K. Naiya, A.K. Bhattacharya, S.K. Das, Removal of Cd(II) from aqueous solutions using clarified sludge, *J. Colloid Interface Sci.*, 325 (2008) 48–56.
- [27] B. Yu, Y. Zhang, A. Shukla, S.S. Shukla, K.L. Dorris, The removal of heavy metals from aqueous solutions by sawdust adsorption-removal of lead and comparison of its adsorption with copper, *J. Hazard. Mater.*, 84 (2001) 83–94.
- [28] G. Bayramoglu, S. Bektas, M.Y. Arica, Biosorption of heavy metal ions on immobilized white-rot fungus, *J. Hazard. Mater.*, 101 (2003) 285–300.
- [29] S. Kalyani, J.A. Priya, P.S. Rao, A. Krishnaiah, Removal of copper and nickel from aqueous solutions using chitosan-coated on perlite as biosorbent, *Sep. Sci. Technol.*, 40 (2005) 1483–1495.
- [30] B. Bayat, Comparative study of sorption properties of Turkish fly ashes I, The case of nickel(II), copper(II), and zinc(II), *J. Hazard. Mater.*, 95 (2002) 251–273.
- [31] J.Y. Huang, Z.W. Wu, L.W. Chen, Y.B. Sun, Surface complexation modeling of adsorption of Cd(II) on graphene oxides, *J. Mol. Liq.*, 209 (2015) 753–758.
- [32] A.P. Davis, V. Bhatnagar, Adsorption of cadmium and humic acid onto hematite, *Chemosphere*, 30 (1995) 243–256.
- [33] Y.S. Ho, G. McKay, Pseudo-second-order model for sorption processes, *Process Biochem.*, 34 (1999) 451–465.
- [34] W.J. Weber Jr., J.C. Morris, Kinetics of adsorption on carbon from solution, *J. Sanitary Eng. Div.*, 89 (1963) 31–60.
- [35] Y.S. Ho, Citation review of Lagergren kinetic rate equation on adsorption reactions, *Scientometrics*, 59 (2004) 171–177.
- [36] P.S. Kumar, K. Ramakrishnan, S.D. Kirupha, S. Sivanesan, Thermodynamic and kinetic studies of cadmium adsorption from aqueous solution onto rice husk, *Braz. J. Chem. Eng.*, 27 (2010) 347–355.
- [37] Y.S. Ho, G. McKay, The kinetics of sorption of divalent metal ions onto Sphagnum moss peat, *Water Res.*, 34 (2000) 735–742.
- [38] W. Liu, J. Zhang, C. Cheng, G. Tian, C. Zhang, Ultrasonic-assisted sodium hypochlorite oxidation of activated carbons for enhanced removal of Co(II) from aqueous solutions, *Chem. Eng. J.*, 175 (2011) 24–32.
- [39] L.Y. Jiang, Q.C. Ye, J.M. Chen, Z. Chen, Y.L. Gu, Preparation of magnetically recoverable bentonite-Fe₃O₄-MnO₂ composite particles for Cd(II) removal from aqueous solutions, *J. Colloid Interface Sci.*, 513 (2018) 748–759.
- [40] H. Wang, X.J. Wang, J.X. Ma, P. Xia, J.F. Zhao, Removal of cadmium(II) from aqueous solution: a comparative study of raw attapulgite clay and a reusable waste-struvite/attapulgite obtained from nutrient-rich wastewater, *J. Hazard. Mater.*, 329 (2017) 66–76.
- [41] J.M. Duan, B. Su, Removal characteristics of Cd(II) from acidic aqueous solution by modified steel-making slag, *Chem. Eng. J.*, 246 (2014) 160–167.
- [42] O. Rahmanian, M.H. Maleki, M. Dinari, Ultrasonically assisted solvothermal synthesis of novel Ni/Al layered double hydroxide for capturing of Cd(II) from contaminated water, *J. Phys. Chem. Solids*, 110 (2017) 195–201.
- [43] M.L. Li, Z.Q. Zhang, R.H. Li, J.J. Wang, A. Ali, Removal of Pb(II) and Cd(II) ions from aqueous solution by thiosemicarbazide modified chitosan, *Int. J. Biol. Macromol.*, 86 (2016) 876–884.
- [44] X.H. Zhu, J. Li, J.H. Luo, Y. Jin, D. Zheng, Removal of cadmium (II) from aqueous solution by a new adsorbent of

- fluor-hydroxyapatite composites, *J. Taiwan Inst. Chem. Eng.*, 70 (2017) 200–208.
- [45] H.M.F. Freundlich, Über die adsorption in lösungen, *Z. Phys. Chem.*, 57 (1906) 385–470.
- [46] I. Langmuir, The adsorption of gases on plane surfaces of glass, mica, and platinum, *J. Am. Chem. Soc.*, 40 (1918) 1361–1403.
- [47] G. Rangel-Porras, J.B. Garcia-Magno, M.P. Gonzalez-Munoz, Lead and cadmium immobilization on calcitic limestone materials, *Desalination*, 262 (2010) 1–10.
- [48] L. Luo, C. Ma, Y. Ma, S. Zhang, J. Lv, M. Cui, New insights into the sorption mechanism of cadmium on red mud, *Environ. Pollut.*, 159 (2011) 1108–1113.
- [49] M. Ulmanu, E. Maranon, Y. Fernandez, L. Castrillon, I. Anger, D. Dumitriu, Removal of copper and cadmium ions from diluted aqueous solutions by low-cost and waste material adsorbents, *Water Air Soil Pollut.*, 142 (2003) 357–373.
- [50] A. Sonmezay, O.M. Salim, N. Bektas, Adsorption of lead and cadmium ions from aqueous solutions using manganoxide minerals, *Trans. Nonferrous Met. Soc. China*, 22 (2012) 3131–3139.
- [51] E. Alvarez-Ayuso, A. Garcia-Sanchez, Removal of heavy metals from wastewaters by natural and Na-exchanged bentonites, *Clays Clay Miner.*, 51 (2003) 475–480.
- [52] E.I. Unuabonah, K.O. Adebawale, Adsorption of Pb(II), and Cd(II) from aqueous solutions onto sodium tetraborate-modified kaolinite clay: equilibrium and thermodynamic studies, *Hydrometallurgy*, 93 (2008) 1–9.
- [53] S.S. Gupta, K.G. Bhattacharyya, Immobilization of Pb(II), Cd(II), and Ni(II) ions on kaolinite and montmorillonite surfaces from aqueous medium, *J. Environ. Manage.*, 87 (2008) 46–58.
- [54] Y. Liu, Is the free energy change of adsorption correctly calculated?, *J. Chem. Eng. Data*, 54 (2009) 1981–1985.
- [55] D.L. Zhao, S.H. Chen, S.B. Yang, X. Yang, S.T. Yang, Investigation of the sorption behavior of Cd(II) on GMZ bentonite as affected by solution chemistry, *Chem. Eng. J.*, 166 (2011) 1010–1016.
- [56] N. Kataria, V.K. Garg, Green synthesis of Fe₃O₄ nanoparticles loaded sawdust carbon for cadmium(II) removal from water: regeneration and mechanism, *Chemosphere*, 208 (2018) 818–828.